

# BENK: the Beran Estimator with Neural Kernels for Estimating the Heterogeneous Treatment Effect

Stanislav R. Kirpichenko, Lev V. Utkin, Andrei V. Konstantinov  
 Peter the Great St.Petersburg Polytechnic University  
 St.Petersburg, Russia

e-mail: kirpichenko.sr@gmail.com, lev.utkin@gmail.com, andrue.konst@gmail.com

## Abstract

A method for estimating the conditional average treatment effect under condition of censored time-to-event data called BENK (the Beran Estimator with Neural Kernels) is proposed. The main idea behind the method is to apply the Beran estimator for estimating the survival functions of controls and treatments. Instead of typical kernel functions in the Beran estimator, it is proposed to implement kernels in the form of neural networks of a specific form called the neural kernels. The conditional average treatment effect is estimated by using the survival functions as outcomes of the control and treatment neural networks which consists of a set of neural kernels with shared parameters. The neural kernels are more flexible and can accurately model a complex location structure of feature vectors. Various numerical simulation experiments illustrate BENK and compare it with the well-known T-learner, S-learner and X-learner for several types of the control and treatment outcome functions based on the Cox models, the random survival forest and the Nadaraya-Watson regression with Gaussian kernels. The code of proposed algorithms implementing BENK is available in <https://github.com/Stasychbr/BENK>.

*Keywords:* treatment effect, survival analysis, Nadaraya-Watson regression, Beran estimator, neural network, meta-learner.

## 1 Introduction

Survival analysis is an important and fundamental tool for modelling applications using time-to-event data [1] which can be encountered in medicine, reliability, safety, finance, etc. This is a reason why many machine learning models have been developed to deal with time-to-event data and to solve the corresponding problems in the framework of survival analysis [2, 3, 4]. The crucial peculiarity of time-to-event data is that a training set consists of censored and uncensored observations. When time-to-event exceeds the duration of observation, we have a censored observation. When an event is observed, i.e., time-to-event coincides with the duration of the observation, we deal with an uncensored observation.

Many survival models are available to cover various cases of the time-to-event probability distributions and their parameters [3]. One of the important models is the Cox proportional hazards model [5] which can be regarded as a regression semi-parametric model. There are also many parametric and non-parametric models. If to consider the machine learning survival models, then it is important to point out that, in contrast to other machine learning models, their outcomes are functions, for example, survival functions, hazard functions, cumulative hazard functions. For instance, the well-known effective model called the random survival forest (RSFs) [6] predicts survival

functions (SFs) or cumulative hazard functions.

An important area of the survival model application is the problem of the treatment effect estimation, which is often solved in the framework of machine learning problems [7, 8]. The treatment effect shows how a treatment may be efficient depending on characteristics of a patient. The problem is solved by dividing patients into two groups called treatment and control such that patients from the different groups can be compared. One of the popular measures of the efficient treatment used in machine learning models is the average treatment effect (ATE) [9], which is estimated on the basis of observed data about patients as the mean difference between outcomes of patients from the treatment and control groups.

Due to the difference between characteristics of patients and between their responses to a particular treatment, the treatment effect is measured by the conditional average treatment effect (CATE) which is defined as the mean difference between outcomes of patients from the treatment and control groups conditional on a patient feature vector [10]. In fact, most methods of the CATE estimation are based on constructing two regression models for controls and treatments. However, two difficulties of the CATE estimation can be met. The first one is that the treatment group is usually very small. Therefore, many machine learning models cannot be accurately trained on the small datasets. The second difficulty is fundamental. Each patient cannot be simultaneously in the treatment and control groups, i.e., we either observe the patient outcome under treatment or control, but never both [11]. Nevertheless, to overcome the difficulties, many methods for estimating CATE have been proposed and developed due to importance of the problem in many areas [12, 13, 14, 15, 16, 17, 18, 19].

One of the approaches for constructing regression models for controls and treatments is the application of the Nadaraya-Watson kernel regression [20, 21], which uses standard kernel functions, for instance, the Gaussian, uniform, or Epanechnikov kernels. In order to avoid selecting a standard kernel, Konstantinov et al. [22] proposed to implement kernels and the whole Nadaraya-Watson kernel regression by using a set of identical neural subnetworks with shared parameters with a specific way of the network training. The corresponding method called TNW-CATE (the Trainable Nadaraya-Watson regression for CATE) is based on an important assumption that domains of the feature vectors from the treatment and control groups are similar. Indeed, we often treat patients after being in the control group, i.e., it is assumed that treated patients came to the treatment group from the control group. The neural kernels (kernels implemented as the neural network) are more flexible, and they can accurately model a complex location structure of feature vectors, for instance, when feature vectors from the control and treatment group are located on the spiral as it is shown in Fig. 1 where small triangular and circle markers correspond to the treatment and control groups, respectively. This is another important peculiarity of TNW-CATE. Results provided in [22] illustrated outperformance of TNW-CATE in comparison with other methods when the treatment group is very small and the feature vectors have complex structure.

Following the ideas of TNW-CATE, we propose the CATE estimation method, called BENK (the Beran Estimator with Neural Kernels), dealing with censored time-to event data. The main idea behind the method is to apply the Beran estimator [23] for training the neural kernels. The Beran estimator allows us to get SFs conditional on the feature vectors, which can be regarded as outcomes of regression survival models for the treatment and control group. The Beran estimator depends on a kernel which is used for estimating. We again propose to implement the kernels by means of neural subnetworks and estimate CATE by using the obtained SFs.

Various numerical experiments illustrate BENK and its peculiarities. They also show that BENK outperforms many well-known meta-models: the T-learner, the S-learner, the X-learner for several control and treatment output functions based on the Cox models, the RSF and the Nadaraya-Watson regression with Gaussian kernels.

The code of the proposed algorithms can be found in <https://github.com/Stasychbr/BENK>.

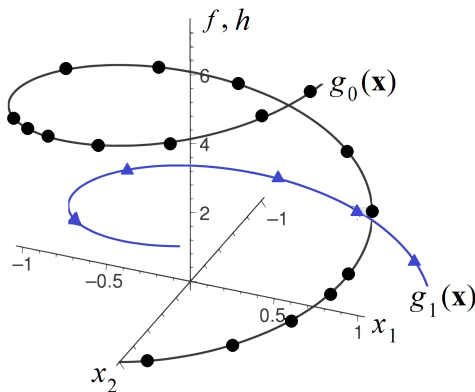


Figure 1: An example of the control  $g_0(\mathbf{x})$  and treatment  $g_1(\mathbf{x})$  functions, which are unknown, and of the control (circle markers) and treatment (triangle markers) data points, which are observed

The paper is organized as follows. Section 2 is a review of the existing CATE estimation models, including CATE estimation survival models, the Nadaraya-Watson regression models and general survival models. A formal statement of the CATE estimation problem is provided in Section 3. The CATE estimation problem in case of censored data is stated in Section 4. The Beran estimator is considered in Section 5. A description of BENK is provided in Section 6. Numerical experiments illustrating BENK and comparing it with other models can be found in Section 7. Concluding remarks are provided in Section 8.

## 2 Related work

**Estimating CATE.** One of the important approaches to implement the personalized medicine [24] is the treatment effect estimation. As a result, many interesting machine learning models have been developed and implemented to estimate CATE. First, we have to point out an approach which uses the Lasso model for estimating CATE [25]. The SVM was also applied to solving the problem [26]. A unified framework for constructing fast tree-growing procedures for solving the CATE problem was provided in [27, 28]. An interesting model for computing CATE was proposed in [14] where the training set is splitting into two subsets such that the first one is used to construct the partition of the data into subpopulations that differ in the magnitude of their treatment effect, and the second subset is used to estimate treatment effects for each subpopulation. The CATE detection problem was considered as a false positive rate control problem in [29]. Alaa and Schaar [13] proposed algorithms for estimating CATE in the context of Bayesian nonparametric inference. Bayesian additive regression trees, a causal forest, and a causal boosting models were compared under condition of binary outcomes in [30]. An orthogonal random forest as an algorithm that combines orthogonalization with generalized random forests for solving the CATE estimation problem was proposed in [31]. McFowland et al. [32] estimated CATE by using the anomaly detection model. A set of meta-algorithms or meta-learners, including the T-learner [33], the S-learner [33], the O-learner [34], the X-learner [33] were studied in [33]. Many other models related to the CATE estimation problem are studied in [35, 36, 37, 24, 38].

The aforementioned models are constructed by using the machine learning methods different from neural networks. However, neural networks became a basis for developing many interesting and efficient models [39, 40, 41, 42, 43, 44, 45, 46, 47].

The next generation of models solving the CATE estimation problem is based on architectures of transformers [48] with the attention operations [49, 50, 51, 52]. The transfer learning technique was successfully applied to the CATE estimation in [53, 54, 55, 11, 56]. Ideas of using the Nadaraya-Watson kernel regression in the CATE estimation were studied in [57, 58]. These ideas can lead to the best results under condition of large numbers of examples in the treatment and control groups. At the same time, a small amount of training data may lead to overfitting and unsatisfactory results. Therefore, a problem of overcoming this possible limitation motivated to introduce a neural network of a special architecture, which implements the trainable kernels in the Nadaraya-Watson regression [22].

**Machine learning models in survival analysis.** Importance of the survival analysis applications can be regarded as one of the reasons for developing many machine learning methods dealing with censored and time-to-event data. A comprehensive review of machine learning survival models is presented in [3]. A large part of models uses the Cox model which can be viewed as a simple and applicable survival model which establish a relationship between covariates and outcomes. Various extensions of the Cox model have been proposed. They can be conditionally divided into two groups. The first group remains the linear relationship of covariates and includes various modifications of the Lasso models [59, 60]. The second group of models relaxes the linear relationship assumption accepted in the Cox model [61, 62].

Many survival models are based on using the RSFs which can be regarded as powerful tools especially when models learn on tabular data [63, 64, 65, 66]. At the same time, there are many survival models based on neural networks [67, 2, 68, 69].

**The Nadaraya-Watson regression in machine learning.** The Nadaraya-Watson regression can be viewed as an effective tool for solving many machine learning tasks [70, 71, 72, 73, 74, 75]. In particular, the Nadaraya-Watson regression was used as a trainable convolution neural network layer in [76]. An interesting approach to simplify the Nadaraya-Watson estimator by approximating the kernel functions produced from data points which are located in the neighborhood of input values was presented by Ito et al. [77]. Noh et al. [78] considered how the Nadaraya-Watson kernel regression can be applied to solve a metric learning model. An application of the Nadaraya-Watson regression to the local explanation, in particular, to the method SHAP, was proposed by Ghalebikesabi et al. [79]. The most important application of the Nadaraya-Watson regression is the attention mechanism explanation, i.e., it can be regarded as a way for explaining ideas of the attention mechanism from the statistics point of view [48, 80].

**Estimating CATE with censored data.** Censored data can be regarded as an important type especially for estimating the treatment effect because many applications are characterized by the time-to-event data as outcomes. This peculiarity is a reason for developing many CATE models dealing with censored data in the framework of survival analysis. In particular, a modification of the survival causal tree method for estimating the CATE based on censored observational data was proposed in [81]. An approach combining a treatment-specific semi-parametric Cox loss with a treatment-balanced deep neural network was studied in [82]. Nagpal et al. [83] presented a latent variable approach to model CATE under assumption that an individual can belong to one of latent clusters with distinct response characteristics. Causal survival forests was introduced in [84], which can be used to estimate CATE under condition of right-censored data. The problem of estimating CATE with focusing on learning (discrete-time) treatment-specific conditional hazard functions was studied in [85]. A three-stage modular design for estimating CATE in the framework of survival analysis was proposed in [86]. A comprehensive simulation study presenting a wide range of settings

describing CATE taking into account the covariate overlap was carried out in [87]. Doubly robust estimation equations were derived in [88] where estimators for the nuisance parameters based on working regression models for the outcome, censoring, and treatment distribution conditional on auxiliary baseline covariates are implemented. Rytgaard et al. [89] presented a data-adaptive estimation procedure for estimation of CATE in a time-to-event setting based on generalized random forests. The authors proposed a two-step procedure for estimation, applying inverse probability weighting to construct time-point specific weighted outcomes as input for the forest. A unified framework for counterfactual inference applicable to survival outcomes and formulating a nonparametric hazard ratio metric for evaluating CATE were proposed in [90].

In spite of many works and results devoted to estimating CATE with censored data, they are mainly based on assumptions of a large amount of examples in the treatment group. Moreover, there are no results implementing the Nadaraya-Watson regression by means of neural networks.

### 3 CATE estimation problem statement

According to the CATE estimation problem, all patients are divided into two groups: control and treatment. Let the control group be the set  $\mathcal{C} = \{(\mathbf{x}_1, f_1), \dots, (\mathbf{x}_c, f_c)\}$  of  $c$  patients such that the  $i$ -th patient is characterized by the feature vector  $\mathbf{x}_i = (x_{i1}, \dots, x_{id}) \in \mathbb{R}^d$  and the  $i$ -th observed outcome  $f_i \in \mathbb{R}$  (time to event, temperature, the blood pressure, etc.). It is also supposed that the treatment group is the set  $\mathcal{T} = \{(\mathbf{y}_1, h_1), \dots, (\mathbf{y}_t, h_t)\}$  of  $t$  patients such that the  $i$ -th patient is characterized by the feature vector  $\mathbf{y}_i = (y_{i1}, \dots, y_{id}) \in \mathbb{R}^d$  and the  $i$ -th observed outcome  $h_i \in \mathbb{R}$ . The indicator of a group for the  $i$ -th patient is denoted as  $T_i \in \{0, 1\}$ , where  $T_i = 0$  ( $T_i = 1$ ) corresponds to the control (treatment) group.

We use different notations  $\mathbf{x}_i$  and  $\mathbf{y}_i$  for controls and treatments in order to avoid additional indices. However, we will use the vector  $\mathbf{z} \in \mathbb{R}^d$  instead of  $\mathbf{x}$  and  $\mathbf{y}$  when estimate the CATE.

Suppose that the potential outcomes of patients from the control and treatment groups are  $F$  and  $H$ , respectively. The treatment effect for a new patient with the feature vector  $\mathbf{z}$  is estimated by the individual treatment effect defined as  $H - F$ . The fundamental problem of computing CATE is that only one of outcomes  $f$  or  $h$  for each patient can be observed. An important assumption of unconfoundedness [91] is used to allow the untreated patients to be used to construct an unbiased counterfactual for the treatment group [92]. According to the assumption, potential outcomes are characteristics of a patient before the patient is assigned to a treatment condition, or formally the treatment assignment  $T$  is independent of the potential outcomes for  $F$  and  $H$  conditional on the feature vector  $\mathbf{z}$ , respectively, which can be written as

$$T \perp \{F, H\} | \mathbf{z}. \quad (1)$$

The second assumption, called the overlap assumption, regards the joint distribution of treatments and covariates. This assumption claims that a positive probability of being both treated and untreated for each value of  $\mathbf{z}$  exists. It is of the form:

$$0 < \Pr\{T = 1 | \mathbf{z}\} < 1. \quad (2)$$

Let  $\mathbf{Z}$  be the random feature vector from  $\mathbb{R}^d$ . The treatment effect is estimated by means of CATE which is defined as the expected difference between two potential outcomes as follows [93]:

$$\tau(\mathbf{z}) = \mathbb{E}[H - F | \mathbf{Z} = \mathbf{z}]. \quad (3)$$

By using the above assumptions, CATE can be rewritten as:

$$\tau(\mathbf{z}) = \mathbb{E}[H | \mathbf{Z} = \mathbf{z}] - \mathbb{E}[F | \mathbf{Z} = \mathbf{z}]. \quad (4)$$

The motivation behind unconfoundedness is that nearby observations in the feature space can be treated as having come from a randomized experiment [94].

Suppose that functions  $g_0(\mathbf{z})$  and  $g_1(\mathbf{z})$  express outcomes of the control and treatment patients, respectively. Then they can be written as follows:

$$f = g_0(\mathbf{z}) + \varepsilon, \quad h = g_1(\mathbf{z}) + \varepsilon, \quad (5)$$

where  $\varepsilon$  is a noise governed by the normal distribution with the zero expectation.

The above implies that CATE can be estimated as:

$$\tau(\mathbf{z}) = g_1(\mathbf{z}) - g_0(\mathbf{z}). \quad (6)$$

An example illustrating controls (circle markers), treatments (triangle markers) and the corresponding unknown function  $g_0$  and  $g_1$  are shown Fig. 1.

## 4 CATE with censored data

Before considering the CATE estimation problem with censored data, we introduce basic statements of survival analysis. Let us define the training set  $D_0$  which consists of  $c$  triplets  $(\mathbf{x}_i, \delta_i, f_i)$ ,  $i = 1, \dots, c$ , where  $\mathbf{x}_i^T = (x_{i1}, \dots, x_{id})$  is the feature vector characterizing the  $i$ -th patient from the control group;  $f_i$  is the time to the event concerning the  $i$ -th control patient;  $\delta_i \in \{0, 1\}$  is the indicator of censored or uncensored observations. If  $\delta_i = 1$ , then the event of interest is observed (the uncensored observation). If  $\delta_i = 0$ , then we have the censored observation. Only the right censoring is considered when the observed survival time is less than or equal to the true survival time. Many applications of survival analysis deal with the right censored observations [3]. The main goal of the survival machine learning modelling is to use set  $D_0$  to estimate probabilistic characteristics of time  $F$  to the event of interest for a new patient with the feature vector  $\mathbf{z}$ .

In the same way, we define the training set  $D_1$  which consists of  $d$  triplets  $(\mathbf{y}_i, \gamma_i, h_i)$ ,  $i = 1, \dots, s$ , where  $\mathbf{y}_i^T = (y_{i1}, \dots, y_{id})$  is the feature vector characterizing the  $i$ -th patient from the treatment group;  $h_i$  is the time to the event concerning the  $i$ -th treatment patient;  $\gamma_i \in \{0, 1\}$  is the indicator of censoring.

The survival function (SF), denoted  $S(t|\mathbf{z})$ , can be regarded as an important concept in survival analysis. It represents the probability of surviving of a patient with the feature vector  $\mathbf{z}$  up to time  $t$  that is  $S(t|\mathbf{z}) = \Pr\{T > t|\mathbf{z}\}$ . The hazard function, denoted  $\lambda(t|\mathbf{z})$ , can be viewed as another concept in survival analysis. It is defined as the rate of event at time  $t$  given that no event occurred before time  $t$ . It is expressed through the SF as follows:

$$\lambda(t|\mathbf{z}) = -\frac{d}{dt} \ln S(t|\mathbf{z}). \quad (7)$$

The integral of the hazard function, denoted  $H(t|\mathbf{x})$ , is called the cumulative hazard function and can be interpreted as the probability of an event at time  $t$  given survival until time  $t$ , i.e.,

$$\Lambda(t|\mathbf{z}) = \int_{-\infty}^t \lambda(r|\mathbf{z}) dr. \quad (8)$$

It is expressed through the SF as follows:

$$\Lambda(t|\mathbf{z}) = -\ln(S(t|\mathbf{z})). \quad (9)$$

The above functions for controls and treatments will be written with indices 0 and 1, respectively, for example,  $S_0(t|\mathbf{z}) = \Pr\{F > t|\mathbf{z}\}$  and  $S_1(t|\mathbf{z}) = \Pr\{H > t|\mathbf{z}\}$ .

In order to compare survival models the Harrell's concordance index or the C-index [95] is usually used. The C-index measures the probability that, in a randomly selected pair of examples, the example that fails first had a worst predicted outcome. It is calculated as the ratio of the number of pairs correctly ordered by the model to the total number of admissible pairs. A pair is not admissible if the events are both right-censored or if the earliest time in the pair is censored. If the C-index is equal to 1, then The corresponding survival model is supposed to be perfect when the C-index is 1. The case when the C-index is 0.5 says that the survival model is the same as random guessing. The case when the C-index is less than 0.5 says that the corresponding model is worse than random guessing.

In contrast to the standard CATE estimation problem statement given in the previous section, the CATE estimation problem with censored data has another statement which is caused by the fact that outcomes in survival analysis are random times to event of interest having some conditional probability distribution. In other words, predictions corresponding to a patient characterizing by vector  $\mathbf{z}$  in survival analysis provided by a survival machine learning model are represented in the form of functions of time, for example, in the form of SF  $S(t|\mathbf{z})$ . This implies that CATE  $\tau(\mathbf{x})$  should be reformulated taking into account the above peculiarity. It is assumed that SFs as well as hazard functions for control and treatment patients estimated by using datasets  $D_0$  and  $D_1$  will have indices 0 and 1, respectively.

The following definitions of CATE in the case of censored data can be found in [96, 97, 98]:

1. Difference in expected lifetimes:  $\tau(\mathbf{z}) = \int_0^{t_{\max}} (S_1(t|\mathbf{z}) - S_0(t|\mathbf{z})) dt = \mathbb{E}\{T_1 - T_0|X = \mathbf{z}\}$ .
2. Difference in SFs:  $\tau(t, \mathbf{z}) = S_1(t|\mathbf{z}) - S_0(t|\mathbf{z})$ .
3. Hazard ratio:  $\tau(t, \mathbf{z}) = \lambda_1(t|\mathbf{z})/\lambda_0(t|\mathbf{z})$ .

We will use the first integral definition of CATE. Let  $0 = t_0 < t_1 < \dots < t_n$  be the distinct times to event of interest which are obtained from the set  $\{f_1, \dots, f_c\} \cup \{h_1, \dots, h_s\}$ . The SF provided by a survival machine learning model is a step function, i.e., it can be represented as  $S(t|\mathbf{z}) = \sum_{j=1}^n S^{(j)}(\mathbf{z}) \cdot \chi_j(t)$ , where  $\chi_j(t)$  is the indicator function taking value 1 if  $t \in [t_{j-1}, t_j]$ ;  $S^{(j)}(\mathbf{z})$  is the value of the SF in interval  $[t_{j-1}, t_j]$ . Hence, there holds

$$\begin{aligned} \tau(\mathbf{z}) &= \int_0^{t_{\max}} (S_1(t|\mathbf{z}) - S_0(t|\mathbf{z})) dt \\ &= \sum_{j=1}^n (S_1^{(j)}(\mathbf{z}) - S_0^{(j)}(\mathbf{z})) (t_j - t_{j-1}). \end{aligned} \quad (10)$$

## 5 Nonparametric estimation of survival functions and CATE

The idea to use the Nadaraya-Watson regression for estimating SFs and other concepts of survival analysis has been proposed by several authors [99, 100, 101, 102, 103]. One of the interesting estimators is the Beran estimator [23] of the SF which is defined as follows:

$$S(t|\mathbf{x}) = \prod_{f_i \leq t} \left\{ 1 - \frac{W(\mathbf{x}, \mathbf{x}_i)}{1 - \sum_{j=1}^{i-1} W(\mathbf{x}, \mathbf{x}_j)} \right\}^{\delta_i}, \quad (11)$$

where  $W(\mathbf{x}, \mathbf{x}_i)$  are the Nadaraya-Watson weights defined as

$$W(\mathbf{x}, \mathbf{x}_i) = \frac{K(\mathbf{x}, \mathbf{x}_i)}{\sum_{j=1}^n K(\mathbf{x}, \mathbf{x}_j)}. \quad (12)$$

The above expression is given for the controls. The same estimator can be written for treatments, but  $\mathbf{x}$ ,  $\delta_i$ ,  $f_i$  is replaced with  $\mathbf{y}$ ,  $\gamma_i$ ,  $h_i$ , respectively.

The Beran estimator can be regarded as a generalization of the Kaplan-Meier estimator because it is reduced to the Kaplan-Meier estimator if the Nadaraya-Watson weights take values  $W(\mathbf{x}, \mathbf{x}_i) = 1/n$ . It is also interesting to note that the product in (11) takes into account only uncensored observations whereas the weights are normalized by using uncensored as well as censored observations.

By using (11) and (10), we can construct a neural network which is trained to implement the weights  $W(\mathbf{z}, \mathbf{x}_i)$ ,  $W(\mathbf{z}, \mathbf{y}_i)$  and to estimate SFs  $S_1(t|\mathbf{z})$  and  $S_0(t|\mathbf{z})$  for computing  $\tau(\mathbf{z})$ .

## 6 Neural network for estimating CATE

Let us consider how the Beran estimator with neural kernels can be implemented by means of a neural network of a special type. Our first aim is to implement kernels  $K(\mathbf{x}, \mathbf{x}_i)$  by means of a neural subnetwork, which is called the neural kernel and is a part of the whole network implementing the Beran estimator. The second aim is to learn this network on the control data. Having the trained kernel, we can apply it to compute the conditional survival function for controls as well as for treatments because the kernels in (11) directly do not depend on times to events  $f_i$  or  $h_i$ . However, in order to train the kernel, we have to train the whole network because the loss function is defined through SF  $S_0(t|\mathbf{x})$  which represents the probability of surviving of a control patient up to time  $t$ , and which is estimated by means of the Beran estimator. This implies that the whole network contains blocks of neural kernels for computing kernels  $K(\mathbf{x}, \mathbf{x}_i)$ , normalization for computing the Nadaraya-Watson weights  $W(\mathbf{x}, \mathbf{x}_i)$  and the Beran estimator in accordance with (11). In order to realize a training procedure of the network, we randomly select a part ( $n$  examples) from all control training examples and form a single specific example from  $n$  selected ones. This random selection is repeated  $N$  times to have  $N$  examples for training.

Having the trained neural kernel, it can be successfully used for computing SF  $S_0(t|\mathbf{z})$  of controls and SF  $S_1(t|\mathbf{z})$  of treatments for arbitrary vectors of features  $\mathbf{z}$  again applying the Beran estimator.

Let us consider the training algorithm in detail. First, we return to the set of  $c$  controls  $\mathcal{C} = \{(\mathbf{x}_i, \delta_i, f_i), i = 1, \dots, c\}$ . For every  $i$  from set  $\{1, \dots, c\}$ , we construct  $N$  subsets  $\mathcal{C}_i^{(r)}$ ,  $r = 1, \dots, N$ , having  $n$  examples randomly selected from  $\mathcal{C} \setminus (\mathbf{x}_i, \delta_i, f_i)$ , which have indices from the index set  $\mathcal{I}^{(r)}$ , i.e., the subsets  $\mathcal{C}_i^{(r)}$  is of the form:

$$\mathcal{C}_i^{(r)} = \{(\mathbf{x}_k^{(r)}, \delta_k^{(r)}, f_k^{(r)}), k \in \mathcal{I}^{(r)}\}, r = 1, \dots, N. \quad (13)$$

Here  $N$  and  $n$  can be regarded as tuning hyperparameters. Upper index  $r$  indicates that the  $r$ -th example  $(\mathbf{x}_k^{(r)}, \delta_k^{(r)}, f_k^{(r)})$  is randomly taken from  $\mathcal{C} \setminus (\mathbf{x}_i, \delta_i, f_i)$ , i.e., there is an example  $(\mathbf{x}_j, \delta_j, f_j)$  from  $\mathcal{C}$  such that  $\mathbf{x}_k^{(r)} = \mathbf{x}_j$ ,  $\delta_k^{(r)} = \delta_j$ ,  $f_k^{(r)} = f_j$ . Each subsets  $\mathcal{C}_i^{(r)}$  jointly with  $(\mathbf{x}_i, \delta_i, f_i)$  forms a training example  $\mathbf{a}_i^{(r)}$  for the control network as follows:

$$\mathbf{a}_i^{(r)} = \left( \mathcal{C}_i^{(r)}, \mathbf{x}_i, \delta_i, f_i \right), i = 1, \dots, c, r = 1, \dots, N. \quad (14)$$



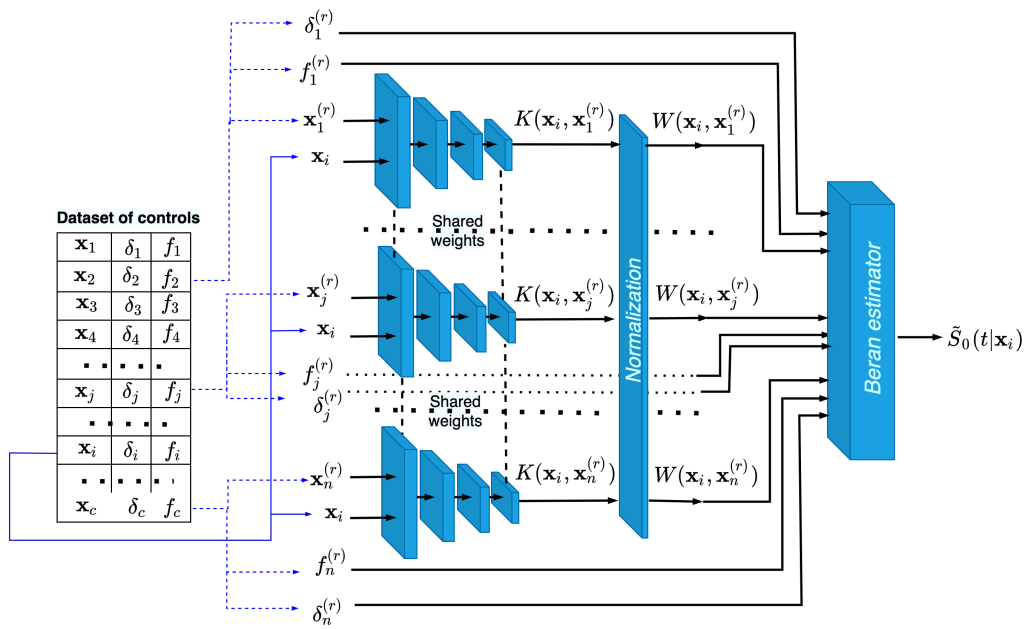


Figure 2: The neural network training on examples  $\mathbf{a}_i^{(r)}$  composed of controls for producing the Beran estimator in the form of SF  $\tilde{S}_0(t|\mathbf{x}_i)$

The number of possible examples  $\mathbf{a}_i^{(r)}$  is  $c \cdot N$ , and these examples will be used for training the neural network whose output is the estimate of SF  $\tilde{S}_0(t|\mathbf{x}_i)$ .

The architecture of the neural network consisting of  $n$  subnetworks which implement the neural kernels is shown in Fig. 2. Examples  $\mathbf{a}_i^{(r)}$  produced from the dataset of controls are fed to the whole neural network such that each pair  $(\mathbf{x}_i, \mathbf{x}_k^{(r)})$ ,  $k \in \mathcal{I}^{(r)}$ , is fed to each subnetwork which implements the kernel function. The output of each subnetwork is kernel  $K(\mathbf{x}_i, \mathbf{x}_k^{(r)})$ . All subnetworks are identical and have shared weights. After normalizing the kernels, we get  $n$  weights  $W(\mathbf{x}_i, \mathbf{x}_k^{(r)})$  which are used to estimate SFs by means of the Beran estimator in (11). The block of the whole neural network implementing the Beran estimator uses all weights  $W(\mathbf{x}_i, \mathbf{x}_k^{(r)})$ ,  $k \in \mathcal{I}^{(r)}$ , and the corresponding values  $\delta_k^{(r)}$  and  $f_k^{(r)}$ ,  $k \in \mathcal{I}^{(r)}$ . As a result, we get SF  $\tilde{S}_0(t|\mathbf{x}_i)$ . In the same way, we compute SFs  $\tilde{S}_0(t|\mathbf{x}_k)$  for all  $k = 1, \dots, c$ . These functions are the basis for training. In fact, the normalization block and the block implementing the Beran estimator are not a real part of the neural network and they are not trained. They need to compute SFs and the corresponding loss functions. However, we introduce these blocks into the presented architecture in order to show that the loss function is determined through the Beran estimator.

According to (10), expected lifetimes are used to compute CATE  $\tau(\mathbf{z})$ . Therefore, the whole network is trained by means of the following loss function:

$$L = \frac{1}{c^* \cdot N} \sum_{i \in \mathcal{C}^*} \sum_{k=1}^N \left( \tilde{E}_k^{(i)} - f_k^{(i)} \right)^2. \quad (15)$$

Here  $\mathcal{C}^*$  is a subset of  $\mathcal{C}$ , which contains only uncensored examples from  $\mathcal{C}$ ;  $c^*$  is the number of elements in  $\mathcal{C}^*$ ;  $f_k^{(i)}$  is the time to event of the  $k$ -th example from the set  $\mathcal{C}^* \setminus (\mathbf{x}_i, \delta_i, f_i)$ ;  $\tilde{E}_k^{(i)}$  is the expected lifetime computed through SF  $\tilde{S}_0(t|\mathbf{x}_k)$  by integrating the SF:

$$\tilde{E}_k^{(i)} = \sum_{j=1}^n (f_j^{(i)} - f_{j-1}^{(i)}) \tilde{S}_0(f_j^{(i)} | \mathbf{x}_k). \quad (16)$$

The sum in (15) is taken over uncensored examples from  $\mathcal{C}$ . However, the Beran estimator uses all examples.

It is important to point out that our aim is to train subnetworks with shared training parameters, which are the neural kernels. By having the trained neural kernels, we can use them to compute kernels  $K(\mathbf{z}, \mathbf{x}_i)$  and  $K(\mathbf{z}, \mathbf{y}_i)$  and then to compute estimates of SFs  $\tilde{S}_0(t|\mathbf{z})$  and  $\tilde{S}_1(t|\mathbf{z})$  for controls and treatments, respectively, i.e., we realize the idea to transfer tasks from the control group to the treatment group. Let  $t_1^{(0)} < t_2^{(0)} < \dots < t_c^{(0)}$  and  $t_1^{(1)} < t_2^{(1)} < \dots < t_s^{(1)}$  be the ordered time moments corresponding to times  $f_1, \dots, f_c$  and  $h_1, \dots, h_s$ , respectively. Then CATE  $\tau(\mathbf{z})$  can be computed through SFs  $S_1(t|\mathbf{z})$  and  $S_0(t|\mathbf{z})$  again by using the Beran estimators with the trained neural kernels, i.e., there holds in accordance with (10):

$$\tau(\mathbf{z}) = \sum_{j=1}^s (t_j^{(1)} - t_{j-1}^{(1)}) \tilde{S}_1^{(j)}(\mathbf{z}) - \sum_{k=1}^c (t_k^{(0)} - t_{k-1}^{(0)}) \tilde{S}_0^{(k)}(\mathbf{z}), \quad (17)$$

where  $\tilde{S}_1^{(j)}(\mathbf{z})$  is the estimation of the SF of treatments in interval  $[t_{j-1}^{(1)}, t_j^{(1)})$ ;  $\tilde{S}_0^{(k)}(\mathbf{z})$  is the estimation of SF of controls in interval  $[t_{k-1}^{(0)}, t_k^{(0)})$ ; it is assumed  $t_0^{(0)} = t_0^{(1)} = 0$ .

The illustration of neural networks predicting  $K(\mathbf{z}, \mathbf{x}_i)$  and  $K(\mathbf{z}, \mathbf{y}_i)$  for a new vector  $\mathbf{z}$  of feature are shown in Fig. 3. It can be seen from Fig. 3 that the first neural network consists of  $c$  subnetworks

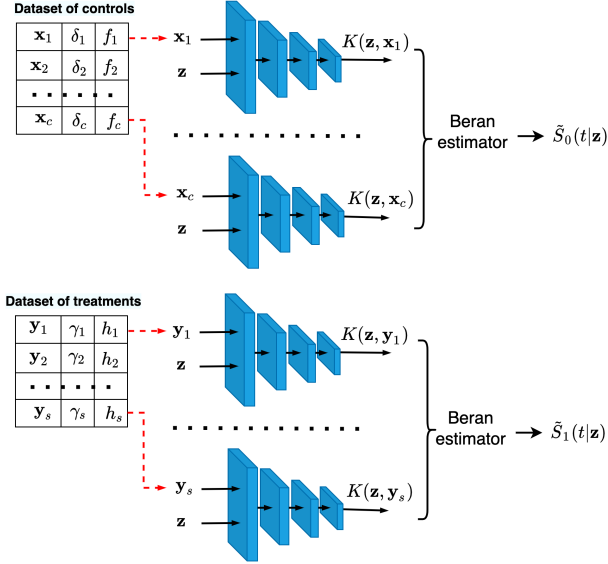


Figure 3: Neural networks consisting of the  $c$  and  $s$  trained neural kernels predicting new values of kernels  $K(\mathbf{z}, \mathbf{x}_i)$  and  $K(\mathbf{z}, \mathbf{y}_i)$  corresponding to controls and treatments for computing estimates of  $S_1(t|\mathbf{z})$  and  $S_0(t|\mathbf{z})$ , respectively

such that pairs of vectors  $(\mathbf{z}, \mathbf{x}_i)$ ,  $i = 1, \dots, c$ , are fed to the subnetworks where  $\mathbf{x}_i$  is taken from the dataset of controls. Predictions of the first neural network are  $c$  kernels  $K(\mathbf{z}, \mathbf{x}_i)$  which are used to compute  $\tilde{S}_0(t|\mathbf{z})$  by means of the Beran estimator (11). The same architecture has the neural network for predicting kernels  $K(\mathbf{z}, \mathbf{y}_i)$  used for estimating the treatment SF  $\tilde{S}_1(t|\mathbf{z})$ . This network consists of  $s$  subnetworks and uses vectors  $\mathbf{y}_i$  from the dataset of treatments. After computing estimates  $\tilde{S}_0(t|\mathbf{z})$  and  $\tilde{S}_1(t|\mathbf{z})$ , we can find CATE  $\tau(\mathbf{z})$ .

Phases of training and computing CATE  $\tau(\mathbf{x})$  by means of neural kernels are schematically shown as Algorithms 1 and 2, respectively.

## 7 Numerical experiments

Numerical experiments for studying BENK and its comparison with available models are performed by using simulated datasets because the true CATEs are unknown due to the fundamental problem of the causal inference for real data [11]. This implies that control and treatment datasets are randomly generated in accordance with predefined outcome functions. Nine models

### 7.1 CATE estimators for comparison and their parameters

For investigating BENK and its comparison, we use nine models which can be united in three groups (the T-learner, the S-learner, the X-learner) such that every group is based on three base models for estimating SFs (the RSF, the Cox model, the Nadaraya-Watson kernel regression and the Beran estimator). The models are given below in terms of survival models.

---

**Algorithm 1** The algorithm for training neural kernels

---

**Require:** Datasets  $\mathcal{C}$  of  $c$  controls and  $\mathcal{T}$  of  $s$  treatments, number  $N$  of generated subsets  $\mathcal{C}_i^{(r)}$  of  $\mathcal{C}$ , number of examples in generated subsets  $n$

**Ensure:** Neural kernels  $K(\cdot, \cdot)$  for their use in the Beran estimator for control and treatment data

- 1: **for**  $i = 1, i \leq c$  **do**
  - 2:   **for**  $r = 1, r \leq N$  **do**
  - 3:     Generate subset  $\mathcal{C}_i^{(r)} \subset \mathcal{C} \setminus (\mathbf{x}_i, y_i)$
  - 4:     Form example  $\mathbf{a}_i^{(r)} = (\mathcal{C}_i^{(r)}, \mathbf{x}_i, \delta_i, f_i)$
  - 5:   **end for**
  - 6: **end for**
  - 7: Train the weight sharing neural network with the loss function given in (15) on the set of examples  $\mathbf{a}_i^{(r)}$
- 

---

**Algorithm 2** The algorithm for computing CATE for a new feature vector  $\mathbf{z}$

---

**Require:** Trained neural kernels, datasets  $\mathcal{C}$  and  $\mathcal{T}$ , testing example  $\mathbf{z}$

**Ensure:** CATE  $\tau(\mathbf{x})$

- 1: **for**  $i = 1, i \leq c$  **do**
  - 2:   Form pair  $(\mathbf{z}, \mathbf{x}_i)$  of vectors by using the dataset  $\mathcal{C}$  of controls
  - 3:   Feed pair  $(\mathbf{z}, \mathbf{x}_i)$  to the trained neural kernel and predict  $K(\mathbf{z}, \mathbf{x}_i)$
  - 4: **end for**
  - 5: **for**  $i = 1, i \leq s$  **do**
  - 6:   Form pair  $(\mathbf{z}, \mathbf{y}_i)$  of vectors by using the dataset  $\mathcal{T}$  of treatments
  - 7:   Feed pair  $(\mathbf{z}, \mathbf{y}_i)$  to the trained neural kernel and predict  $K(\mathbf{z}, \mathbf{y}_i)$
  - 8: **end for**
  - 9: Compute  $W(\mathbf{z}, \mathbf{x}_i), i = 1, \dots, c, W(\mathbf{z}, \mathbf{y}_i), i = 1, \dots, s$
  - 10: Estimate  $\tilde{S}_0(t|\mathbf{x}_k)$  and  $\tilde{S}_1(t|\mathbf{y}_k)$  using (11)
  - 11: Compute  $\tau(\mathbf{x})$  using (17)
-

1. The T-learner [33] is a model which estimates the control SF  $S_0(t|\mathbf{z})$  and the treatment SF  $S_1(t|\mathbf{z})$  for every  $\mathbf{z}$ . The CATE in this case is defined in accordance with (10).
2. The S-learner [33] is a model which estimates SF  $S(t|\mathbf{z}, T)$  instead of  $S_0(t|\mathbf{z})$  and  $S_1(t|\mathbf{z})$  where the treatment assignment indicator  $T_i \in \{0, 1\}$  is included as an additional feature to the feature vector  $\mathbf{z}_i$ . As a result, we have a modified dataset

$$\mathcal{D} = \{(\mathbf{z}_1^*, \delta_1, f_1), \dots, (\mathbf{z}_c^*, \delta_c, f_c), (\mathbf{z}_{c+1}^*, \gamma_1, h_1), \dots, (\mathbf{z}_{c+s}^*, \gamma_s, h_s)\}, \quad (18)$$

where  $\mathbf{z}_i^* = (\mathbf{x}_i, T_i) \in \mathbb{R}^{d+1}$  if  $T_i = 0$ ,  $i = 1, \dots, c$ , and  $\mathbf{z}_{c+i}^* = (\mathbf{y}_i, T_i) \in \mathbb{R}^{d+1}$  if  $T_i = 1$ ,  $i = 1, \dots, t$ . The CATE is determined as

$$\tau(\mathbf{z}) = \sum_{j=1}^s (t_j^{(1)} - t_{j-1}^{(1)}) \tilde{S}^{(j)}(\mathbf{z}, 1) - \sum_{k=1}^c (t_k^{(0)} - t_{k-1}^{(0)}) \tilde{S}^{(k)}(\mathbf{z}, 0). \quad (19)$$

3. The X-learner [33] is based on computing the so-called imputed treatment effects and is represented in the following three steps. The outcome functions  $g_0(\mathbf{x})$  and  $g_1(\mathbf{y})$  are estimated using a regression algorithm. Second, the imputed treatment effects are computed as follows:

$$D_1(\mathbf{y}_i) = h_i - g_0(\mathbf{y}_i), \quad D_0(\mathbf{x}_i) = g_1(\mathbf{x}_i) - f_i. \quad (20)$$

Third, two regression functions  $\tau_1(\mathbf{y})$  and  $\tau_0(\mathbf{x})$  are estimated for imputed treatment effects  $D_1(\mathbf{y})$  and  $D_0(\mathbf{x})$ , respectively. CATE for a point  $\mathbf{z}$  is defined as a weighted linear combination of the functions  $\tau_1(\mathbf{z})$  and  $\tau_0(\mathbf{z})$  as  $\tau(\mathbf{z}) = \alpha\tau_0(\mathbf{z}) + (1 - \alpha)\tau_1(\mathbf{z})$ , where  $\alpha \in [0, 1]$  is a weight which is equal to the ratio of treated patients [11]. The original X-learner does not deal with censored data. Therefore, we propose a simple survival modification of the X-learner. It is assumed that  $g_0(\mathbf{y}_i)$  and  $g_1(\mathbf{x}_i)$  are expectations  $E_0(\mathbf{y}_i)$  and  $E_1(\mathbf{x}_i)$  of times to event corresponding to control and treatment data, respectively. Expectations  $E_0(\mathbf{y}_i)$  and  $E_1(\mathbf{x}_i)$  are computed by means of one of the algorithms for determining estimates of SFs  $S_0(t|\mathbf{z})$  and  $S_1(t|\mathbf{z})$ .

Estimation of SFs  $S_0(t|\mathbf{z})$  and  $S_1(t|\mathbf{z})$  as well as  $S(t|\mathbf{z}, T)$  is carried out by means of using the following survival regression algorithms:

1. The RSF [6]. It is used as the base regressor to implement other models due to two main reasons. Parameters of random forests used in experiments are the following:
  - numbers of trees are 50, 100, 200;
  - depths are 2, 4, 6;
  - the smallest values of examples which fall in a leaf are 1 example, 10%, 20% of the training set.

The above values for the hyperparameters are tested, choosing those leading to the best results.

2. The Cox proportional hazards model [5]. It is used with the regularization term with the coefficient taking values 0.1, 0.5, 1, 2, 5.

Table 1: Notations of the models depending on meta-learners and base models

	Meta-model		
Survival regression algorithms	T-learner	S-learner	X-learner
Nadaraya-Watson regression	<b>T-NW</b>	<b>S-NW</b>	<b>X-NW</b>
Cox model	<b>T-Cox</b>	<b>S-Cox</b>	<b>X-Cox</b>
RSF	<b>T-SF</b>	<b>S-SF</b>	<b>X-SF</b>

3. The Nadaraya-Watson kernel regression [20, 21] using the standard Gaussian kernel as the base regression model. In fact, this regression determines SFs by means of the Beran estimator. In contrast to the proposed BENK model, we use the standard Gaussian kernel for determining the attention weights. Values  $10^i$ ,  $i = -3, \dots, 3$ , and also values 0.5, 5, 50, 200, 500, 700 of the bandwidth parameter of the Gaussian kernel are tested, choosing those leading to the best results.

In sum, we have 9 models for comparison whose notations are given in Table 1.

## 7.2 Generating synthetic datasets

We consider two ways for generating random survival times used in numerical experiments. The first way of generating is the same as it has been done in [22]. All numerical experiments are represented on the basis of simulated datasets such that vectors of features are generated by means of three functions: the spiral function, the logarithmic function, the power function. The idea to use these functions stems from the goal to get complex structures of data, which are poorly processed by many standard methods. The above functions are defined through a parameter  $t$  as follows:

1. **Spiral functions:** Two feature vectors having dimensionality  $d$  and located on the Archimedean spirals are defined for even  $d$  as

$$\mathbf{x} = (t \sin(t), t \cos(t), \dots, t \sin(t \cdot d/2), t \cos(t \cdot d/2)), \quad (21)$$

and for odd  $d$  as

$$\mathbf{x} = (t \sin(t), t \cos(t), \dots, t \sin(t \cdot \lceil d/2 \rceil)). \quad (22)$$

Parameter  $t$  is uniformly generated from interval  $[0, 10]$  for controls as well as for treatments.

2. **Logarithmic functions:** The feature vectors are logarithms of parameter  $t$  represented as follows:

$$\mathbf{x} = (a_1 \ln(t), a_2 \ln(t), \dots, a_d \ln(t)). \quad (23)$$

Values of parameters  $a_1, \dots, a_d$  for performing numerical experiments with logarithmic functions are uniformly generated from intervals  $[-4, -1] \cup [1, 4]$  for controls as well as for treatments. Values of  $t$  are uniformly generated from interval  $[0.5, 5]$ .

3. **Power functions:** Features are represented as powers of  $t$ . For arbitrary  $d$  (the number of features), the feature vector is represented as

$$\mathbf{x} = (t^{1/\sqrt{d}}, t^{2/\sqrt{d}}, \dots, t^{d/\sqrt{d}}). \quad (24)$$

It should be noted that the generating model may lead to almost linear features with  $t$  when  $0.8 < i/\sqrt{d} < 1.6$ . To complicate the feature vectors, we replace the feature vectors with

these parameters with the Gaussian noise having the unit standard deviation and the zero expectation, i.e.,  $x_i \sim \mathcal{N}(0, 1)$ . Values of  $t$  are uniformly generated from interval  $[0, 10]$ .

For feature vectors  $\mathbf{x}$  and  $\mathbf{y}$  from control and treatment group, times to events  $f$  and  $h$  are generated by using a modification of the Cox model generator [104] as follows:

$$f = -\ln(0.02)/(0.1 \cdot \exp(0.5 \cdot t)), \quad (25)$$

$$h = -\ln(0.3)/(0.1 \cdot \exp(0.15 \cdot t)), \quad (26)$$

where  $t$  has been generated when vectors  $\mathbf{x}$  for the spiral, logarithmic and power functions were determined.

This way for generating  $f$  and  $g$  is in agreement with the Cox model. Hence, we can use the Cox model as a base model among RSFs and the Nadaraya-Watson regression with Gaussian kernels in numerical experiments.

The number of censored data, denoted as  $p$ , is taken 25% of all observations. Hence, parameters  $\delta_i$  and  $\gamma_i$  are generated from the binomial distribution with probabilities  $\Pr\{\delta_i = 1\} = \Pr\{\gamma_i = 1\} = 0.75$ ,  $\Pr\{\delta_i = 0\} = \Pr\{\gamma_i = 0\} = 0.25$ .

The root mean squared error (RMSE) as a measure of the regression model accuracy is used. The RMSE is computed by using 1000 randomly selected feature vectors  $\mathbf{z}$ . The proportion of treatments and controls in most experiments is 20% except for experiments investigating how the proportion of treatments impacts on the RMSE, where the proportion of treatments and controls is denoted as  $q$ . For example, if 100 controls are generated for an experiment with  $q = 0.2$ , then 20 treatments are generated in addition to controls such that the total number of examples is 120. The generated feature vectors in all experiments consist of 10 features. To select optimal hyperparameters of all regressors, additional validation examples are generated such that the number of controls is 50% of the training examples from the control group. The validation examples are not used for training.

Numerical results are obtained under condition that there is some noise  $\varepsilon$  which is added to functions  $g_0$  and  $g_1$  or to  $f$  and  $h$  as it is depicted in Fig. 4. The noise is generated in accordance with the normal distribution with the zero mean and the standard deviation  $\sigma$  such that  $\varepsilon$  is defined as the proportion of  $3\sigma$  and the mean values of  $f$  and  $h$ . Most numerical experiments are performed under condition  $\varepsilon = 0.05$ . However, a part of experiments illustrate how the noise impact on the CATE prediction. In these experiments, different values of  $\varepsilon$  are used to study how the noise impacts on predictions of different models and BENK.

### 7.3 Study of the BENK properties

In all pictures illustrating results of numerical experiments, dotted curves correspond to the T-learner (triangle markers), the S-learner (triangle markers), the X-learner (the circle marker) under condition of using the Nadaraya-Watson regression with the Gaussian kernel. Dash-and-dot curves correspond to the Cox models. Dashed curves with the same markers correspond to the same models implemented by using RSFs. The solid curve with cross markers corresponds to BENK.

First, we study different CATE estimators by different numbers  $c$  of control taking values 100, 200, 300, 500, 1000. The number of treatments is determined as 20% of the number of controls. Values of  $n$  are  $0.2 \cdot c$ . Fig. 5 illustrates how RMSE of the CATE values depends on the number  $c$  of controls for different estimators when different functions are used for generating examples. Left pictures in Fig. 5 show the difference between BENK and models T-NW, S-NW, X-NW. Central pictures show similar dependencies when models T-Cox, S-Cox, X-Cox are used. Right pictures illustrate the relationship between CATE values predicted by BENK, T-SF, S-SF, X-SF by different

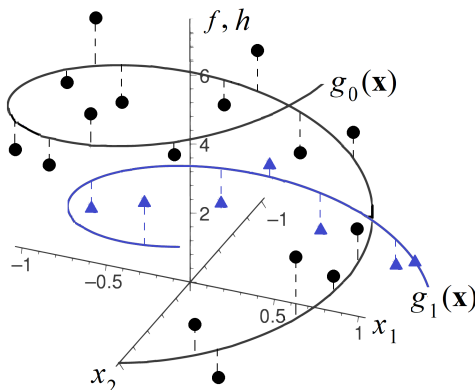


Figure 4: Illustration of the noise added to functions  $g_0(\mathbf{x})$  and  $g_1(\mathbf{x})$

values  $c$ . It can be seen from Fig. 5 that the proposed model BENK provides better results in comparison with other models. The largest relative difference between BENK and other models can be observed when the feature vectors are generated in accordance with the spiral function. This function produces the most complex data structure such that the studied models cannot cope with it. On the other hand, it follows from Fig. 5, illustrating the predicted CATE values for the case of the logarithmic generating function, that models T-NW, S-NW, X-NW provide comparative and sometimes better results than BENK. This is due to usage of the Gaussian kernels which better adjust to the logarithmic locations of feature vectors. The same can be said about models T-Cox, S-Cox, X-Cox based on the Cox model.

It is important to remind that the above numerical results are obtained under condition that noise  $\varepsilon$  is 5%. Therefore, the next question is how the CATE estimators depend on the parameter  $\varepsilon$ . Numerical results illustrating how the noise impact on the CATE estimators for the spiral and power generating functions are shown in Fig. 6. It can be seen from Fig. 6 that the relative difference between the model RMSE measures obtained for the spiral generating function is not change with increase of the noise. However, one can see that this difference increases then the power function is used for generating the feature vectors. In all cases, we again observe outperforming results provided by BENK.

Another interesting question is how the CATE estimators depend on the proportion  $q$  of treatments and controls in the training set. The corresponding numerical results are shown in Fig. 7 for the spiral generating function. One can see from Fig. 7 that improvement of the RMSE is sufficient in comparison with other CATE estimators when  $q$  is changed from 10% to 20%. Moreover, we again observe the outperformance of BENK in comparison with other estimators. It should be noted that similar results take place when other generating functions (logarithmic and power) are used.

In the previous experiments, the amount of censored data was taken  $p = 25\%$  of all observations. However, it is interesting to study how this amount impacts on the RMSE of the CATE estimators. Fig. 8 illustrates the corresponding dependences when the spiral generating function is used. It can be seen from Fig. 8 that RMSE measures of all estimators, including BENK, increase with the amount of censored data.

Figs. 5-8 can be viewed as qualitative results of comparing different estimators. Table 2 aims to



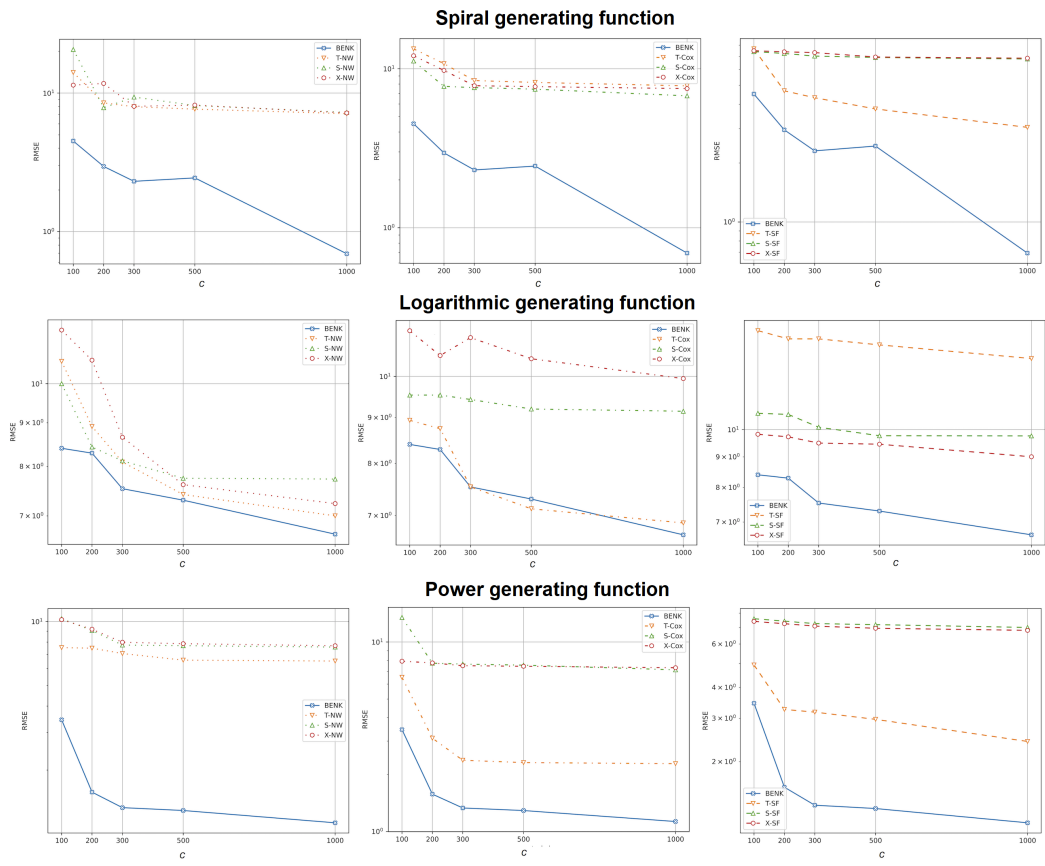


Figure 5: RMSE of the predicted CATE values as a function of the number of controls when the spiral, logarithmic and power functions are used for generating instances, and CATE is computed by using the Nadaraya-Watson regression (left pictures), the Cox model (central pictures), the RSF (right pictures)

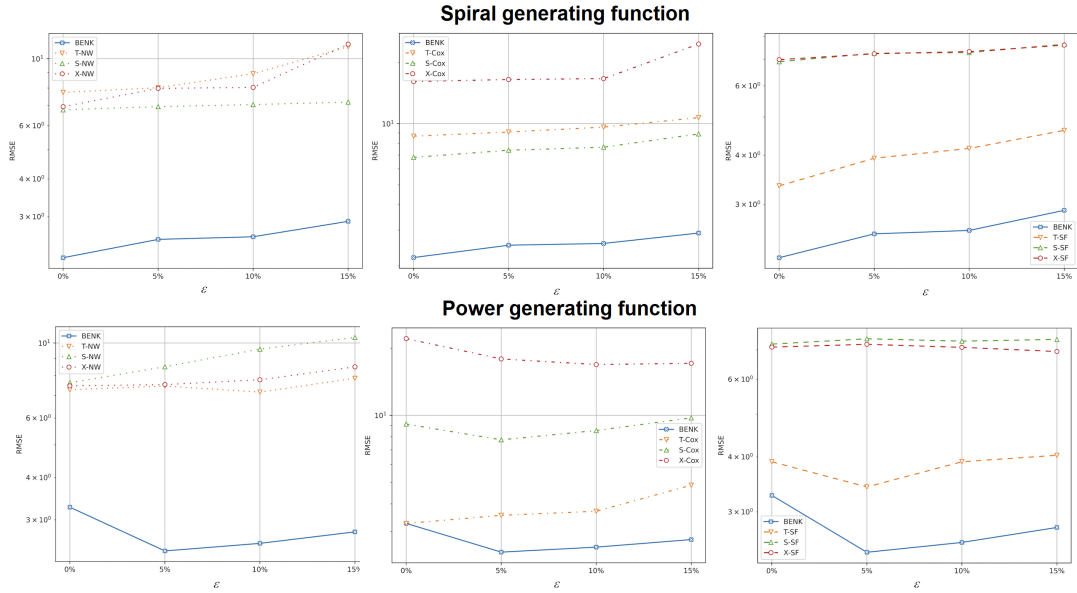


Figure 6: RMSE of the predicted CATE values as functions of the noise value  $\varepsilon$  of controls and treatments when the spiral and power functions are used for generating examples for models: BENK, T-NW, S-NW, X-NW (the left picture) and BENK, T-Cox, S-Cox, X-Cox (the central picture) and BENK, T-SF, S-Cox, X-Cox (the right picture)

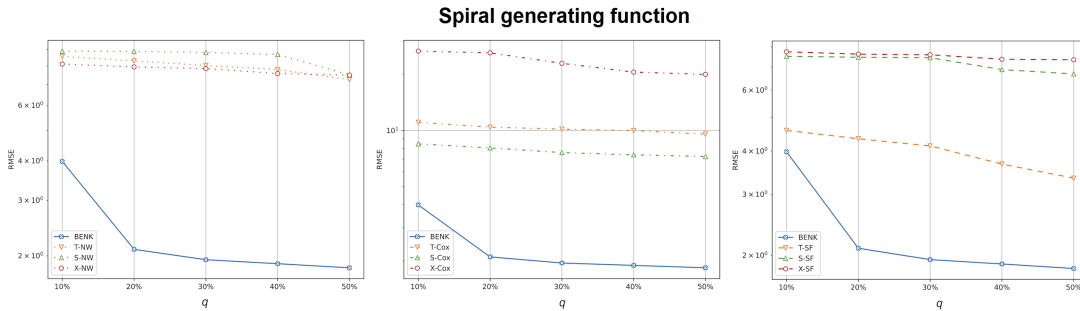


Figure 7: RMSE of the predicted CATE values as functions of on the proportion  $q$  of treatments and controls when the spiral function is used for generating examples for models: BENK, T-NW, S-NW, X-NW (the left picture) and BENK, T-Cox, S-Cox, X-Cox (the central picture) and BENK, T-SF, S-Cox, X-Cox (the right picture)

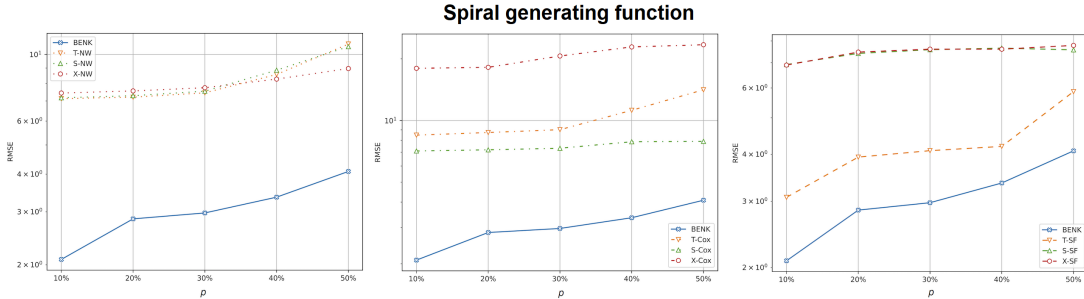


Figure 8: RMSE of the predicted CATE values as functions of on the ratio  $p$  of censored data when the spiral function is used for generating examples for models: BENK, T-NW, S-NW, X-NW (the left picture) and BENK, T-Cox, S-Cox, X-Cox (the central picture) and BENK, T-SF, S-Cox, X-Cox (the right picture)

Table 2: The RMSE values of CATE for different models by different generating functions

Model	Generating functions		
	Spiral	Logarithmic	Power
T-NW	9.984	7.223	7.361
S-NW	7.387	8.978	7.565
X-NW	9.257	9.339	7.199
T-Cox	12.28	6.824	3.312
S-Cox	7.221	6.807	7.412
X-Cox	14.67	9.419	11.91
T-SF	7.245	7.205	5.113
S-SF	7.276	7.104	7.094
X-SF	6.754	9.297	7.875
BENK	<b>6.215</b>	<b>5.456</b>	<b>2.518</b>

quantitatively compare results under the following conditions:  $c = 200$ ,  $s = 60$ ,  $p = 0.3$ ,  $m = 20$ ,  $N = 1000$ ,  $\varepsilon = 0.1$ . One can see from Table 2 that BENK provides ouperforming results.

It should be noted that we did not provide results of various deep neural network extensions of the CATE estimators because they have not been successful. The problem is that neural networks require a large amount of data for training and the considered small datasets have led the networks to overfitting. That is why we studied models which provide satisfactory predictions under condition of small data.

## 8 Conclusion

BENK as a new method for solving the CATE problem under censored data has been presented. It extends the idea behind TNW-CATE proposed in [22] to the case of censored data. In spite of many similar parts of TNW-CATE and BENK they are different because BENK is based on using the Beran estimator for training and can be successfully applied to survival analysis of controls and treatments. However, TNW-CATE and BENK use the same idea to train neural kernels implemented

as neural networks instead of used standard kernels.

It is also interesting to point out that BENK does not require to have a large dataset for training though the neural network is used for implementing the kernels. This is due to a special way which is proposed to train the network and considers pairs of examples from the control group for training like the Siamese neural networks. Our experiments have illustrated the outperforming characteristics of BENK. At the same time, we have to point out some disadvantages of BENK. First, it has many tuning parameters, including parameters of the neural network, parameters of training  $n$  and  $N$ , such that the training time may be sufficiently increased in comparison with other methods of solving the CATE problem. Second, BENK assumes that the feature vector domains are similar for controls and treatments. It does not mean that they have to totally coincide, but the corresponding difference of domains should not be very large. A method which could take into account a possible difference between the feature vector domains for controls and treatments can be regarded as a direction for further research. An idea behind the method is to combine the domain adaptation models and BENK.

Another direction for further research is to study robust versions of BENK when there are anomalous observations which may impact on training the neural network. An idea behind the robust version is to use attention weights for feature vectors, but also to introduce additional attention weights for predictions.

It should be noted that the Beran estimator is one of several estimators which are used in survival analysis. Moreover, we have studied only the difference in expected lifetimes as a definition of CATE in the case of censored data. There are other definitions, for instance, the difference in SFs and the hazard ratio, which may lead to more interesting models. Therefore, the BENK implementations and studies by using other estimators and definitions of CATE can be also considered as directions for further research.

## References

- [1] D. Hosmer, S. Lemeshow, and S. May. *Applied Survival Analysis: Regression Modeling of Time to Event Data*. John Wiley & Sons, New Jersey, 2008.
- [2] J.L. Katzman, U. Shaham, A. Cloninger, J. Bates, T. Jiang, and Y. Kluger. Deepsurv: Personalized treatment recommender system using a Cox proportional hazards deep neural network. *BMC medical research methodology*, 18(24):1–12, 2018.
- [3] P. Wang, Y. Li, and C.K. Reddy. Machine learning for survival analysis: A survey. *ACM Computing Surveys (CSUR)*, 51(6):1–36, 2019.
- [4] L. Zhao and D. Feng. Dnnsurv: Deep neural networks for survival analysis using pseudo values. arXiv:1908.02337v2, March 2020.
- [5] D.R. Cox. Regression models and life-tables. *Journal of the Royal Statistical Society, Series B (Methodological)*, 34(2):187–220, 1972.
- [6] H. Ishwaran and U.B. Kogalur. Random survival forests for r. *R News*, 7(2):25–31, 2007.
- [7] M. Lu, S. Sadiq, D.J. Feaster, and H. Ishwaran. Estimating individual treatment effect in observational data using random forest methods. arXiv:1701.05306v2, Jan 2017.
- [8] U. Shalit, F.D. Johansson, and D.A. Sontag. Estimating individual treatment effect: generalization bounds and algorithms. In *Proceedings of the 34th International Conference on Machine Learning (ICML 2017)*, volume PMLR 70, pages 3076–3085, Sydney, Australia, 2017.

- [9] Y. Fan, J. Lv, and J. Wang. DNN: A two-scale distributional tale of heterogeneous treatment effect inference. arXiv:1808.08469v1, Aug 2018.
- [10] S. Wager and S. Athey. Estimation and inference of heterogeneous treatment effects using random forests. arXiv:1510.0434, 2015.
- [11] S.R. Kunzel, B.C. Stadie, N. Vemuri, V. Ramakrishnan, J.S. Sekhon, and P. Abbeel. Transfer learning for estimating causal effects using neural networks. arXiv:1808.07804v1, Aug 2018.
- [12] arXiv:2205.14714. Heterogeneous treatment effects estimation: When machine learning meets multiple treatment regime. N. Acharki and J. Garnier and A. Bertonecello and R. Lugo, May 2022.
- [13] Ahmed Alaa and Mihaela van der Schaar. Limits of estimating heterogeneous treatment effects: Guidelines for practical algorithm design. In *Proceedings of the 35th International Conference on Machine Learning*, volume 80 of *Proceedings of Machine Learning Research*, pages 129–138, Stockholmsmässan, Stockholm Sweden, 2018. PMLR.
- [14] S. Athey and G. Imbens. Recursive partitioning for heterogeneous causal effects. *Proceedings of the National Academy of Sciences*, pages 1–8, 6 2016.
- [15] T. Hatt, J. Berrevoets, A. Curth, S. Feuerriegel, and M. van der Schaar. Combining observational and randomized data for estimating heterogeneous treatment effects. arXiv:2202.12891, Feb 2022.
- [16] Hao Jiang, Peng Qi, Jingying Zhou, Jack Zhou, and Sharath Rao. A short survey on forest based heterogeneous treatment effect estimation methods: Meta-learners and specific models. In *2021 IEEE International Conference on Big Data (Big Data)*, pages 3006–3012. IEEE, 2021.
- [17] S.R. Kunzel, J.S. Sekhon, P.J. Bickel, and Bin Yu. Metalearners for estimating heterogeneous treatment effects using machine learning. *PNAS*, 116(10):4156–4165, 2019.
- [18] Lili Wu and Shu Yang. Integrative learner of heterogeneous treatment effects combining experimental and observational studies. In *Proceedings of the First Conference on Causal Learning and Reasoning (CLEaR 2022)*, pages 1–23, <https://openreview.net/pdf?id=Q102xPpYV-B>, 2022.
- [19] Weijia Zhang, Jiuyong Li, and Lin Liu. A unified survey of treatment effect heterogeneity modelling and uplift modelling. *ACM Computing Surveys*, 54(8):1–36, 2022.
- [20] E.A. Nadaraya. On estimating regression. *Theory of Probability & Its Applications*, 9(1):141–142, 1964.
- [21] G.S. Watson. Smooth regression analysis. *Sankhya: The Indian Journal of Statistics, Series A*, pages 359–372, 1964.
- [22] A.V. Konstantinov, S.R. Kirpichenko, and L.V. Utkin. Heterogeneous treatment effect with trained kernels of the Nadaraya-Watson regression. arXiv:2207.09139, Jul 2022.
- [23] R. Beran. Nonparametric regression with randomly censored survival data. Technical report, University of California, Berkeley, 1981.

- [24] S. Powers, J. Qian, K. Jung, A. Schuler, N.H. Shah, T. Hastie, and R. Tibshirani. Some methods for heterogeneous treatment effect estimation in high-dimensions some methods for heterogeneous treatment effect estimation in high-dimensions. arXiv:1707.00102v1, Jul 2017.
- [25] X.J. Jeng, W. Lu, and H. Peng. High-dimensional inference for personalized treatment decision. *Electronic Journal of Statistics*, 12:12 2074–2089, 2018.
- [26] X. Zhou, N. Mayer-Hamblett, U. Khan, and M.R. Kosorok. Residual weighted learning for estimating individualized treatment rules. *Journal of the American Statistical Association*, 112(517):169–187, 2017.
- [27] S. Athey, J. Tibshirani, and S. Wager. Solving heterogeneous estimating equations with gradient forests. arXiv:1610.01271, Oct 2016.
- [28] S. Athey, J. Tibshirani, and S. Wager. Generalized random forests. arXiv:1610.0171v4, Apr 2018.
- [29] Y. Xie, N. Chen, and X. Shi. False discovery rate controlled heterogeneous treatment effect detection for online controlled experiments. arXiv:1808.04904v1, Aug 2018.
- [30] T. Wendling, K. Jung, A. Callahan, A. Schuler, N.H. Shah, and B. Gallego. Comparing methods for estimation of heterogeneous treatment effects using observational data from health care databases. *Statistics in Medicine*, pages 1–16, 2018.
- [31] M. Oprescu, V. Syrgkanis, and Z.S. Wu. Orthogonal random forest for heterogeneous treatment effect estimation. arXiv:1806.03467v2, Jul 2018.
- [32] E. McFowland III, S. Somanchi, and D.B. Neill. Efficient discovery of heterogeneous treatment effects in randomized experiments via anomalous pattern detection. arXiv:1803.09159v2, Jun 2018.
- [33] S.R. Kunzel, J.S. Sekhona, P.J. Bickel, and B. Yu. Meta-learners for estimating heterogeneous treatment effects using machine learning. *Proceedings of the National Academy of Sciences*, 116(10):4156–4165, 2019.
- [34] Y. Wang, P. Wu, Y. Liu, C. Weng, and D. Zeng. Learning optimal individualized treatment rules from electronic health record data. In *IEEE International Conference on Healthcare Informatics (ICHI)*, pages 65–71. IEEE, 2016.
- [35] R. Chen and H. Liu. Heterogeneous treatment effect estimation through deep learning. arXiv:1810.11010v1, Oct 2018.
- [36] J. Grimmer, S. Messing, and S.J. Westwood. Estimating heterogeneous treatment effects and the effects of heterogeneous treatments with ensemble methods. *Political Analysis*, 25(4):413–434, 2017.
- [37] J. Levy, M. van der Laan, A. Hubbard, and R. Pirracchio. A fundamental measure of treatment effect heterogeneity. arXiv:1811.03745v1, Nov 2018.
- [38] L. Yao, C. Lo, I. Nir, S. Tan, A. Evnine, A. Lerer, and A. Peysakhovich. Efficient heterogeneous treatment effect estimation with multiple experiments and multiple outcomes. arXiv:2206.04907, Jun 2022.

- [39] I. Bica, J. Jordon, and M. van der Schaar. Estimating the effects of continuous-valued interventions using generative adversarial networks. In *Advances in neural information processing systems (NeurIPS)*, volume 33, pages 16434–16445, 2020.
- [40] Peipei Chen, Wei Dong, Xudong Lu, Uzay Kaymak, Kunlun He, and Zhengxing Huang. Deep representation learning for individualized treatment effect estimation using electronic health records. *Journal of Biomedical Informatics*, 100:1–11, 2019. 103303.
- [41] A. Curth and M. van der Schaar. Nonparametric estimation of heterogeneous treatment effects: From theory to learning algorithms. In *International Conference on Artificial Intelligence and Statistics*, pages 1810–1818. PMLR, 2021.
- [42] Xinze Du, Yingying Fan, Jinchi Lv, Tianshu Sun, and P. Vossler. Dimension-free average treatment effect inference with deep neural networks. arXiv:2112.01574, Dec 2021.
- [43] N. Nair, K.S. Gurumoorthy, and D. Mandalapu. Individual treatment effect estimation through controlled neural network training in two stages. arXiv:2201.08559, Jan 2022.
- [44] Lizhen Nie, Mao Ye, Qiang Liu, and D. Nicolae. Vcnet and functional targeted regularization for learning causal effects of continuous treatments. In *International Conference on Learning Representations (ICLR 2021)*, pages 1–24, 2021.
- [45] S. Parbhoo, S. Bauer, and P. Schwab. Ncore: Neural counterfactual representation learning for combinations of treatments. arXiv:2103.11175, Mar 2021.
- [46] Tian Qin, Tian-Zuo Wang, and Zhi-Hua Zhou. Budgeted heterogeneous treatment effect estimation. In *Proceedings of the 38th International Conference on Machine Learning, PMLR*, volume 139, pages 8693–8702, 2021.
- [47] P. Schwab, L. Linhardt, S. Bauer, J.M. Buhmann, and W. Karlen. Learning counterfactual representations for estimating individual dose-response curves. In *Proceedings of the AAAI Conference on Artificial Intelligence*, volume 34, pages 5612–5619, 2020.
- [48] S. Chaudhari, V. Mithal, G. Polatkan, and R. Ramanath. An attentive survey of attention models. arXiv:1904.02874, Apr 2019.
- [49] Zhenyu Guo, Shuai Zheng, Zhizhe Liu, Kun Yan, and Zhenfeng Zhu. Cetransformer: Casual effect estimation via transformer based representation learning. In *Pattern Recognition and Computer Vision. PRCV 2021*, volume 13022 of *Lecture Notes in Computer Science*, pages 524–535. Springer, Cham, 2021.
- [50] V. Melnychuk, D. Frauen, and S. Feuerriegel. Causal transformer for estimating counterfactual outcomes. arXiv:2204.07258, Apr 2022.
- [51] Yi-Fan Zhang, Hanlin Zhang, Z.C. Lipton, Li Erran Li, and Eric P. Xing. Can transformers be strong treatment effect estimators? arXiv:2202.01336, Feb 2022.
- [52] Yi-Fan Zhang, Hanlin Zhang, Z.C. Lipton, Li Erran Li, and Eric P. Xing. Exploring transformer backbones for heterogeneous treatment effect estimation. arXiv:2202.01336, May 2022.
- [53] R. Aoki and M. Ester. Causal inference from small high-dimensional datasets. arXiv:2205.09281, May 2022.

- [54] Wenshuo Guo, Serena Wang, Peng Ding, Yixin Wang, and M.I. Jordan. Multi-source causal inference using control variates. arXiv:2103.16689, Mar 2021.
- [55] S.R. Kunzel, B.C. Stadie, N. Vemuri, V. Ramakrishnan, J.S. Sekhon, and P. Abbeel. Transfer learning for estimating causal effects using neural networks. arXiv:1808.07804, Aug 2018.
- [56] Guanglin Zhou, Lina Yao, Xiwei Xu, Chen Wang, and Liming Zhu. Learning to infer counterfactuals: Meta-learning for estimating multiple imbalanced treatment effects. arXiv:2208.06748, Aug 2022.
- [57] G.W. Imbens. Nonparametric estimation of average treatment effects under exogeneity: A review. *Review of Economics and Statistics*, 86(1):4–29, 2004.
- [58] J. Park, U. Shalit, B. Scholkopf, and K. Muandet. Conditional distributional treatment effect with kernel conditional mean embeddings and u-statistic regression. In *Proceedings of the 38 th International Conference on Machine Learning, PMLR*, volume 139, pages 8401–8412, 2021.
- [59] S. Kaneko, A. Hirakawa, and C. Hamada. Enhancing the lasso approach for developing a survival prediction model based on gene expression data. *Computational and Mathematical Methods in Medicine*, 2015(Article ID 259474):1–7, 2015.
- [60] D.M. Witten and R. Tibshirani. Survival analysis with high-dimensional covariates. *Statistical Methods in Medical Research*, 19(1):29–51, 2010.
- [61] D. Faraggi and R. Simon. A neural network model for survival data. *Statistics in medicine*, 14(1):73–82, 1995.
- [62] A. Widodo and B.-S. Yang. Machine health prognostics using survival probability and support vector machine. *Expert Systems with Applications*, 38(7):8430–8437, 2011.
- [63] N.A. Ibrahim, A. Kudus, I. Daud, and M.R. Abu Bakar. Decision tree for competing risks survival probability in breast cancer study. *International Journal Of Biological and Medical Research*, 3(1):25–29, 2008.
- [64] U.B. Mogensen, H. Ishwaran, and T.A. Gerds. Evaluating random forests for survival analysis using prediction error curves. *Journal of Statistical Software*, 50(11):1–23, 2012.
- [65] H. Wang and L. Zhou. Random survival forest with space extensions for censored data. *Artificial intelligence in medicine*, 79:52–61, 2017.
- [66] M.N. Wright, T. Dankowski, and A. Ziegler. Unbiased split variable selection for random survival forests using maximally selected rank statistics. *Statistics in Medicine*, 36(8):1272–1284, 2017.
- [67] C. Haarburger, P. Weitz, O. Rippel, and D. Merhof. Image-based survival analysis for lung cancer patients using CNNs. arXiv:1808.09679v1, Aug 2018.
- [68] R. Ranganath, A. Perotte, N. Elhadad, and D. Blei. Deep survival analysis. In *Proceedings of the 1st Machine Learning for Healthcare Conference*, volume 56, pages 101–114, Northeastern University, Boston, MA, USA, 2016. PMLR.
- [69] X. Zhu, J. Yao, and J. Huang. Deep convolutional neural network for survival analysis with pathological images. In *2016 IEEE International Conference on Bioinformatics and Biomedicine*, pages 544–547. IEEE, 2016.



- [70] D. Conn and G. Li. An oracle property of the Nadaraya-Watson kernel estimator for high-dimensional nonparametric regression. *Scandinavian Journal of Statistics*, 46(3):735–764, 2019.
- [71] R. Hanafusa and T. Okadome. Bayesian kernel regression for noisy inputs based on Nadaraya-Watson estimator constructed from noiseless training data. *Advances in Data Science and Adaptive Analysis*, 12(1):2050004–1–2050004–17, 2020.
- [72] A.V. Konstantinov, L.V. Utkin, and S.R. Kirpichenko. AGBoost: Attention-based modification of gradient boosting machine. In *31st Conference of Open Innovations Association (FRUCT)*, pages 96–101. IEEE, 2022.
- [73] Fanghui Liu, Xiaolin Huang, Chen Gong, Jie Yang, and Li Li. Learning data-adaptive nonparametric kernels. *Journal of Machine Learning Research*, 21:1–39, 2020.
- [74] X. Liu, Y. Min, L. Chen, X. Zhang, and C. Feng. Data-driven transient stability assessment based on kernel regression and distance metric learning. *Journal of Modern Power Systems and Clean Energy*, 9(1):27–36, 2021.
- [75] Jianhua Xiao, Zhiyang Xiang, Dong Wang, and Zhu Xiao. Nonparametric kernel smoother on topology learning neural networks for incremental and ensemble regression. *Neural Computing and Applications*, 31:2621–2633, 2019.
- [76] A.B. Szczołka, D.I. Shakir, D. Ravi, M.J. Clarkson, S.P. Pereira, and T. Vercauteren. Learning from irregularly sampled data for endomicroscopy super-resolution: a comparative study of sparse and dense approaches. *International Journal of Computer Assisted Radiology and Surgery*, 15:1167–1175, 2020.
- [77] T. Ito, N. Hamada, K. Ohori, and H. Higuchi. A fast approximation of the nadaraya-watson regression with the k-nearest neighbor crossover kernel. In *2020 7th International Conference on Soft Computing & Machine Intelligence (ISCFMI)*, pages 39–44, 2020.
- [78] Y.-K. Noh, M. Sugiyama, K.-E. Kim, F. Park, and D.D. Lee. Generative local metric learning for kernel regression. In *Advances in Neural Information Processing Systems 30 (NIPS 2017)*, volume 30, pages 1–11, 2017.
- [79] S. Ghalebikesabi, L. Ter-Minassian, K. Diaz-Ordaz, and C. Holmes. On locality of local explanation models. In *35th Conference on Neural Information Processing Systems (NeurIPS 2021)*, pages 1–13, 2021.
- [80] A. Zhang, Z.C. Lipton, M. Li, and A.J. Smola. Dive into deep learning. *arXiv:2106.11342*, Jun 2021.
- [81] W. Zhang, T.D. Le, L. Liu, Z.-H. Zhou, and J. Li. Mining heterogeneous causal effects for personalized cancer treatment. *Bioinformatics*, 33(15):2372–2378, 2017.
- [82] S. Schrod, A. Schäfer, S. Solbrig, R. Lohmayer, W. Gronwald, P.J. Oefner, T. Beissbarth, R. Spang, H.U. Zacharias, and M. Altenbuchinger. Bites: Balanced individual treatment effect for survival data. *arXiv:2201.03448*, Jan 2022.
- [83] C. Nagpal, M. Goswami, K. Dufendach, and A. Dubrawski. Counterfactual phenotyping with censored time-to-events. *arXiv:2202.11089*, Feb 2022.

- [84] Yifan Cui, M.R. Kosorok, E. Sverdrup, S. Wager, and Ruoqing Zhu. Estimating heterogeneous treatment effects with right-censored data via causal survival forests. arXiv:2001.09887, Jan 2020.
- [85] M. van der Schaar A. Curth, Changhee Lee. Survite: Learning heterogeneous treatment effects from time-to-event data. In *Proceedings of the 35th Conference on Neural Information Processing Systems (NeurIPS 2021)*, pages 1–14, 2021.
- [86] Jie Zhu and B. Gallego. Targeted estimation of heterogeneous treatment effect in observational survival analysis. *Journal of Biomedical Informatics*, 107(103474):1–10, 2020.
- [87] Liangyuan Hu, Jiayi Ji, and Fan Li. Estimating heterogeneous survival treatment effect in observational data using machine learning. *Statistics in Medicine*, 40:4691–4713, 2021.
- [88] B.M.H. Ozenne, T.H. Scheike, L. Stark, and T.A. Gerds. On the estimation of average treatment effects with right-censored time to event outcome and competing risks. *Biometrical Journal*, 62:751–763, 2020.
- [89] H.C.W. Rytgaard, C.T. Ekstrom, L.V. Kessing, and T.A. Gerds. Ranking of average treatment effects with generalized random forests for time-to-event outcomes. arXiv:2104.13028, Apr 2021.
- [90] P. Chapfuwa, S. Assaad, Shuxi Zeng, M.J. Pencina, L. Carin, and R. Henao. Enabling counterfactual survival analysis with balanced representations. In *CHIL '21: Proceedings of the Conference on Health, Inference, and Learning*, pages 133–145. ACM, 2021.
- [91] P.R. Rosenbaum and D.B. Rubin. The central role of the propensity score in observational studies for causal effects. *Biometrika*, 70(1):41–55, 1983.
- [92] G.W. Imbens. Nonparametric estimation of average treatment effects under exogeneity: A review. *Review of Economics and Statistics*, 86(1):4–29, 2004.
- [93] D.B. Rubin. Causal inference using potential outcomes: Design, modeling, decisions. *Journal of the American Statistical Association*, 100(469):322–331, 2005.
- [94] S. Wager and S. Athey. Estimation and inference of heterogeneous treatment effects using random forests. arXiv:1510.04342v4, Jul 2017.
- [95] F. Harrell, R. Califf, D. Pryor, K. Lee, and R. Rosati. Evaluating the yield of medical tests. *Journal of the American Medical Association*, 247:2543–2546, 1982.
- [96] P. Chapfuwa, S. Assaad, S. Zeng, M. Pencina, L. Carin, and R. Henao. Survival analysis meets counterfactual inference. arXiv:2006.07756, Jun 2020.
- [97] L. Trinquart, J. Jacot, S.C. Conner, and R. Porcher. Comparison of treatment effects measured by the hazard ratio and by the ratio of restricted mean survival times in oncology randomized controlled trials. *Journal of Clinical Oncology*, 34(15):1813–1819, 2016.
- [98] Lihui Zhao, Lu Tian, Hajime Uno, S.D. Solomon, M.A. Pfeffer, J.S. Schindler, and Lee Jen Wei. Utilizing the integrated difference of two survival functions to quantify the treatment contrast for designing, monitoring, and analyzing a comparative clinical study. *Clinical trials*, 9(5):570–577, 2012.

- [99] S. Bobrowski, Hong Chen, M. Doring, U. Jensen, and W. Schinkothe. Estimation of the lifetime distribution of mechatronic systems in the presence of a covariate: A comparison among parametric, semiparametric and nonparametric models. *Reliability Engineering & System Safety*, 139:105–112, 2015.
- [100] K.E. Gneyou. A strong linear representation for the maximum conditional hazard rate estimator in survival analysis. *Journal of Multivariate Analysis*, 128:10–18, 2014.
- [101] R. Pelaez, R. Cao, and J.M. Vilar. Nonparametric estimation of the conditional survival function with double smoothing. *Journal of Nonparametric Statistics*, 2022. Published online.
- [102] I. Selingerova, S. Katina, and I. Horova. Comparison of parametric and semiparametric survival regression models with kernel estimation. *Journal of Statistical Computation and Simulation*, 91(13):2717–2739, 2021.
- [103] G. Tutz and L. Pritscher. Nonparametric estimation of discrete hazard functions. *Lifetime Data Analysis*, 2(3):291–308, 1996.
- [104] R. Bender, T. Augustin, and M. Blettner. Generating survival times to simulate cox proportional hazards models. *Statistics in Medicine*, 24(11):1713–1723, 2005.